The critical effects start to be measurable at $(T-T_C)/T_C \sim 10^{-3}$. This behavior is similar to that of the binary diffusion coefficient of two liquids approaching the critical point of separation,[7] which falls to zero as predicted by theory.[8] This similarity is not surprising since there is experimental evidence for a phase separation of impurities in the neighborhood of the critical point of a fluid,[9] arising from the large density fluctuations.

Previous self-diffusion measurements in the critical region have been carried out by a nmr technique on C_2H_6 [10] and on CH_4.[11] While in CH_4, as in Ar, no appreciable change in the critical region was observed, in C_2H_6 a decrease of D amounting to about 50% was found. Such a discrepancy could arise from the technique employed for C_2H_6. In fact, to reduce the proton spin-lattice relaxation time, 1% of O_2 was added to the sample. Bearing in mind the above considerations on the behavior of impurities in the critical region, one should regard these data as diffusion of O_2 in C_2H_6.

Finally, Modena and Ricci have recently reported that the mobility of electrons in He^3 shows a smooth decrease of 30% in the critical region.[12] In these measurements the motion of the electronic bubble is due to the driving force of the applied electric field. Unless a frictional mechanism is assumed for the diffusion in the fluid, the resulting viscous motion of the bubble cannot be compared with a diffusive process. The measurements are in good agreement with the observed behavior of viscosity of CO_2, which increases smoothly in the critical region.[13]

---

*Present address: Department of Chemistry, Brookhaven National Laboratory, Upton, N. Y. 11973.

[1]M. De Paz, B. Turi, and M. L. Klein, to be published.

[2]M. De Paz, in Proceedings of the Fourth Symposium on Thermophysical Properties, Maryland, April, 1967 (to be published).

[3]A. Michels, J. M. Levelt, and W. De Graaf, Physica 25, 659 (1958).

[4]K. Kawasaki, Phys. Rev. 150, 285 (1966).

[5]M. S. Giterman and M. E. Gertsenshtein, Zh. Eksperim. i Teor. Fiz. 50, 1084 (1966) [translation: Soviet Phys.—JETP 23, 722 (1966)].

[6]I. R. Krichevskij, N. E. Khazanova, and L. R. Linshits, Dokl. Akad. Nauk. SSSR 141, 397 (1961); N. E. Khazanova and L. S. Lesnevskaya, Zh. Fiz. Khim. 40 76, 464 (1966).

[7]L. O. Sundelof, Arkiv Kemi 15, 317 (1960); H. L. Lorentzen and B. B. Hansen, Acta Chem. Scand. 11, 893 (1957), and 12, 139 (1958).

[8]M. Fixman, Advan. Chem. Phys. 6, 175 (1964).

[9]D. L. Timrot and K. F. Shuiskaya, Inzh.-Fiz. Zh. Akad. Nauk Belorussk. SSR 10, 176 (1966); Y. R. Chashkin, V. G. Gorubnova, and A. V. Voronel, Zh. Eksperim. i Teor. Fiz. 49, 433 (1965) [translation: Soviet Phys.—JETP 22, 304 (1966)].

[10]J. D. Noble and M. Bloom, Phys. Rev. Letters 14, 250 (1965).

[11]N. J. Trappeniers and P. H. Oosting, Phys. Letters 23, 445 (1966).

[12]I. Modena and F. P. Ricci, Phys. Rev. Letters 19, 347 (1967).

[13]J. Kestin, J. H. Whitelaw, and T. F. Zien, Physica 30, 161 (1964).

SUPPRESSION OF A TWO-STREAM INTERACTION IN A BEAM-PLASMA SYSTEM BY EXTERNAL ac ELECTRIC FIELDS

T. Obiki, R. Itatani, and Y. Otani
Department of Electrical Engineering, Kyoto University, Kyoto, Japan
(Received 13 November 1967)

We report an experimental study of the interactions between ion-acoustic waves excited in a beam-plasma system and externally applied ac electric fields. This ac electric field is introduced into the plasma through a beam modulation. The nonlinear interactions described here are the modulation and asynchronous quenching of the ion-acoustic waves and the subharmonic resonance of the applied signals or so-called parametric resonances.[1]

The experimental arrangement is shown in Fig. 1. A cylindrical discharge tube (made of glass) of the hot-cathode type was used with an electron gun. The accelerating electrode E_3 of the gun in Fig. 1 worked as an anode for the main discharge in pair with the hot cathode K. A plasma was produced by means of a hot-cathode mercury discharge at the current I_d from 1 to 100 mA; the plasma density was in the range 10^8-10^9 cm^{-3} at the background pres-

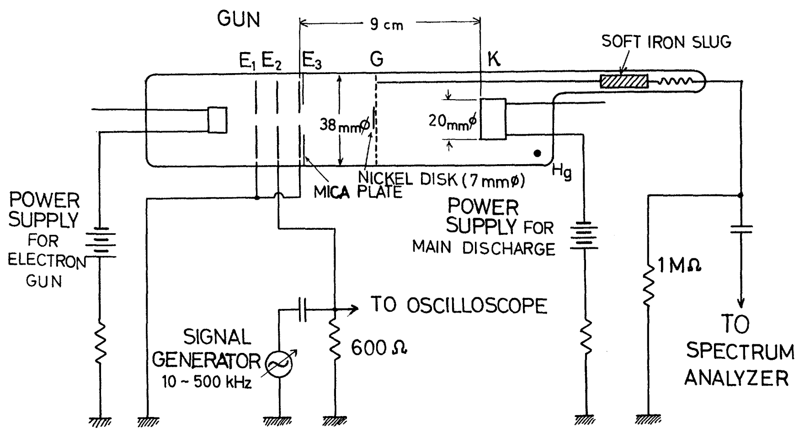

FIG. 1. Experimental tube and test setup.

sure of 10^{-3} mm Hg (at room temperature). The electron beam of 0-100 V in energy V_b, and 0.1-10 mA in beam current I_b, was injected into the plasma along the tube axis through a hole in the anode. An external sinusoidal signal, the frequency range of which is from 20 Hz to 500 kHz, of 0-40 V in peak-to-peak amplitude was applied to the electron beam by the second accelerating electrode E_2 of the gun so as to modulate the beam density. The modulation depth of the beam density was about several tens of percent at the external signal intensity of 20 V. The first and the third electrodes, E_1 and E_3, were grounded lest the applied signal should directly affect the plasma. A movable meshed grid G was inserted between the cathode and the anode in order to detect the fluctuations in the plasma. A small nickel disk was directly mounted on the mesh at the center of the grid in order to stop the electron beam from the gun. The diameter of the beam was about 5 mm. The signals detected by the grid were led to an oscilloscope and a spectrum analyzer.

In this system, no fluctuations were found in some discharge conditions in the absence of the electron beam. When the electron beam of 10-20 V was injected into the plasma without the modulating signal, an ion-acoustic wave of about 60 kHz was excited through the process of a two-stream instability.[2] The beam seems to obey a shifted Maxwellian velocity distribution, and its temperature is nearly equal to the background electron temperature (2-3 eV) of the discharge plasma. These facts were confirmed with the use of the Langmuir probe.

When the modulating signal is applied to the beam, the ion-acoustic oscillation is affected in various ways depending on the amplitude and the frequency of the applied signal. The typical oscillation spectra of the modulated beam-plasma system are shown in Fig. 2. Here

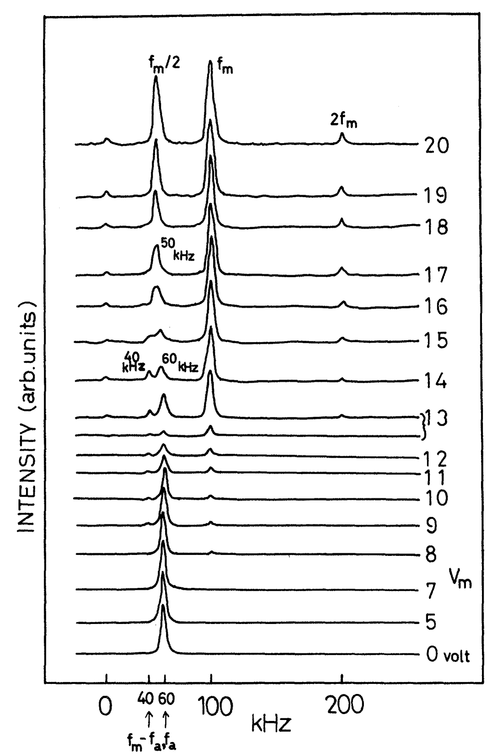

FIG. 2. Typical spectral analyses of a modulated-beam plasma system. The external modulating frequency $f_m = 100$ kHz, the amplitude of which is shown in the figure. The sensitivity of the detecting analyzer was raised at 13 V of V_m.

the amplitude of the modulating signal V_m is varied from 0 to 20 V, while the modulating frequency f_m is maintained at 100 kHz and the ion-acoustic frequency f_a at about 60 kHz. The noticeable phenomenon is found that a new oscillation of frequency $f_m - f_a$ (= 40 kHz) is excited, so the frequency spectra shows the frequency components f_a, f_m, and $f_m - f_a$, as shown in Fig. 2. However, the reason why the frequency component of $f_a + f_m$ does not appear is not clear. The frequency component at about 0 kHz (which is not exactly 0) begins to appear at $V_m \gtrsim 13$ V. This minor component is always found when the ion-acoustic wave is damped; the correspondence or relations between this component and f_a or f_m are not clear.

The amplitude of the ion-acoustic wave decreases with the increase of the modulating signal amplitude.[3] The width of the spectrum of the ion-acoustic oscillation becomes broad and the frequency is slightly shifted. The damping effect of the applied signal is small when the amplitude of the applied signal V_m is less than 10 V, but when V_m exceeds about 10 V, the strong damping effect of the ion-acoustic wave appears. The steady-state (0th order) beam current, beam energy, and the discharge current producing the background plasma were not changed by applying the modulating signal up to about 20 V, but the ion wave is almost completely damped with the modulating signal at or above 17 V.

The solid curve in Fig. 3 represents a dependence of the damping and resonant effect of the existing ion-acoustic wave on the frequency of the modulating signal. The detecting analyzer was tuned at the ion-acoustic frequency f_a, and the output from the analyzer was plotted for several modulating frequencies. The amplitude of the ion-acoustic wave is normalized by the amplitude in the absence of the modulating signal. As is shown by the solid curve in Fig. 3, the asynchronous quenching can be observed at any frequency except for the case when $f_a = nf_m$, where $n = \frac{1}{2}, 1, 2, \cdots$. When the relations $f_a = nf_m$ are satisfied, the ion-acoustic oscillation is recovered in its amplitude. For those frequencies that do not satisfy exactly the relations $f_a = nf_m$, i.e., $f_a \sim nf_m$, the ion-acoustic wave is pulled in or locked to the applied signal when V_m is increased. This phase locking is clearly observed with the use of an oscilloscope. The solid curve also shows two minor peaks at about 40 and

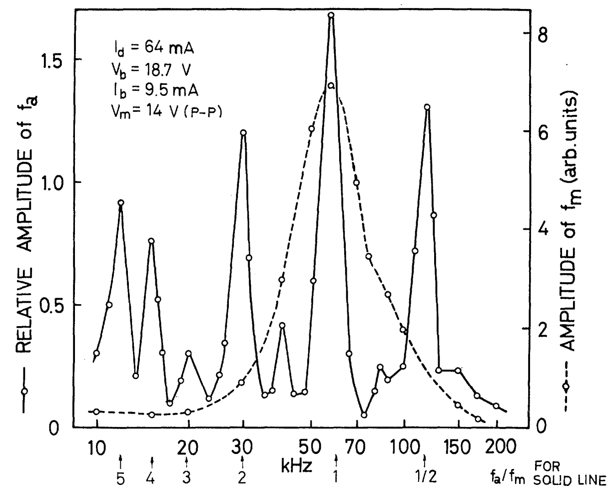

FIG. 3. Solid curve (left scale): Damping and resonance characteristics of the ion waves when the applied signal frequency is varied from 10 to 200 kHz. Broken curve (right scale): Attenuation characteristics of the applied signals detected at the grid. In both cases, the amplitude of the applied signal and other experimental parameters were kept at the same values.

90 kHz. These peaks correspond to $f_a/f_m = \frac{3}{2}$ and $\frac{2}{3}$, respectively. The former seems to appear because f_m (=40 kHz) has a higher harmonic component of frequency $3f_m$ (=120 kHz), which plays the same role when $f_m = 2f_a$ (=120 kHz) is applied. The latter is not clear, although it is very small.

In Fig. 3, the broken curve shows the signal intensity, detected at the grid, of applied signals when f_m is varied with the detecting analyzer tuned to f_m. The broken curve shows the resonant characteristic which resembles that of an ordinary low-quality electrical resonant circuit. The maximum lies at $f_m = f_a$. At frequencies sufficiently higher than f_a, such as $f_m \gtrsim 200$ kHz, the intensity of the applied signal detected at the grid is heavily reduced; but the quenching effect, similar to Fig. 2, on the ion wave is not changed. In other words, the plasma is not much disturbed by such a high-frequency electric field, but the two-stream interaction is suppressed by this high-frequency signal.

The solid curve in Fig. 3 suggests that this system as a whole may be described by the Mathieu-Hill equation[1] in the case of parametric resonances, and that the two-stream microinstability can be suppressed through some nonlinear effect, which is similar to the asynchronous quenching effect in the nonlinear, ordinary differential-equation systems.[4]

---

[1]N. Bogoliubov and Y. A. Mitropolskii, Asymptotic Methods in the Theory of Nonlinear Oscillations (Gordon and Breach Publishers, Inc., New York, 1961), Chap. 3, Sec. 17.

[2]A large number of theoretical and experimental studies have been reported in this field: E. A. Jackson, Phys. Fluids 3, 786 (1960); I. B. Bernstein and R. M. Kulsrud, Phys. Fluids 3, 937 (1960); I. Alexeff and R. V. Neidigh, Phys. Rev. 129, 516 (1963). The oscillations in our experiment were identified with the ion-acoustic waves in the following ways. When the oscillation existed, the frequency of the oscillation as detected at grid G decreased with the increase of the distance L between E_3 and G. The frequency f_a should be, and was observed to be, proportional to L^{-1}. It was also confirmed with the use of a photomultiplier that the ion-acoustic wave was in fact a half-wavelength standing wave between E_2 and G. The phase velocity V_s obtained from the relation between f_a and the wavelength $2(L-2L_s)$, where L_s is a sheath thickness ~0.1 cm, agrees very well with that calculated from probe measurements; for example, $f_a = 60$ kHz, $L-2L_s = 0.8$ cm, then $V_s = 0.96\times10^5$ cm/sec, and the electron temperature $T_e = 2.0$ eV. However, there remains the question whether this ion-acoustic wave is the direct result of a two-stream instability or other mechanism, such as the decay-type instability which was given by V. N. Oraevskii and R. Z. Sagdeev, Zh. Techn. Fiz. 32, 1291 (1962) [translation: Soviet Phys.—Tech. Phys. 7, 955 (1963)], and Y. Ichikawa, Phys. Fluids 9, 1454 (1966), etc.

[3]A similar result has been obtained by E. A. Kornilov et al., Zh. Eksperim. i Teor. Fiz.—Pis'ma Redakt. 3, 354 (1966) [translation: JETP Letters 3, 229 (1966)], who applied microwave signals to an electron beam of about 3 kV for modulation and observed the quenching of the oscillations excited by the beam, but they did not classify the oscillations. The stabilization of a two-stream instability by virtue of the existence of an electric field has been treated theoretically by Yu. M. Aliev and V. P. Silin, Zh. Eksperim. i Teor. Fiz. 48, 901 (1965) [translation: Soviet Phys.—JETP 21, 601 (1965)]. The assumption and the result of this theory are much different from our experiment.

[4]Bogoliubov and Mitropolskii, Ref. 1, Sec. 13.

SUPERFLUIDITY OF LOW-DENSITY FERMION SYSTEMS

D. Fay* and A. Layzer†
Stevens Institute of Technology, Hoboken, New Jersey
(Received 12 December 1967)

In the weak-coupling limit, it has been shown[1] that a system of fermions with purely repulsive forces will be superfluid at zero temperature. This is because the two-particle interaction induced by many-body effects is attractive at the Fermi surface provided that the angular momentum of the pair is sufficiently high. These asymptotic considerations do not permit the specification of the actual momentum of the pairing in the condensed state, much less an accurate estimate of the transition temperature T_c or the magnitude of the energy gap Δ.

We present results here concerning the exact low-density behavior of the pairing interaction U for fermions with arbitrarily strong short-range forces. Only the $T=0$ and $\Delta=0$ limit of U will be considered. It is found that at low densities a pairing interaction can in fact be defined in the BCS manner such that both T_c and Δ are proportional to $\exp[2/\pi m^* \times k_F^{-1} U(k_F, k_F)]$. At low densities, the correction δU induced by many-body effects turns out to be attractive in P states, less strongly attractive in D states, and repulsive in S states. A system of hard spheres at low densities and at $T=0$ should be superfluid in a condensed state with P-state pairing.

Quantitatively we obtain the following results in the limit of low densities. In spite of the strength of the primary interaction v, at low densities δU tends to the expectation value of the induced potential δI on the Fermi surface and on the energy shell. δI is shown in Fig. 1. The blocks T at low densities may be replaced by combinations of ladder diagrams for particle-particle scattering and χ may be replaced by a single particle-hole loop. In the low-density limit with p and k near k_F, $\delta I(p,k)$ turns out to be precisely the same as the lowest-order perturbation value except that, in the final result, $v \to (4\pi/m)\bar{f}_0$, where $\bar{f}_0$ is the zero-energy scattering amplitude ($\bar{f}_0 = R$ for hard spheres). One obtains in this limit

$$\delta I(p,k) = (4\pi/m)^2 \bar{f}_0^{\,2} Q(p+k), \tag{1}$$

$$\delta \bar{U}_l = (2/\pi)(k_F \bar{f}_0)^2 \bar{Q}_l(0)(-1)^l, \tag{2}$$

where $\bar{U} = m k_F^{-1} U$, Q is one-half the usual